^{1}H NMR and EPR Studies of $[M(NH_3)_5(H_2O)](TFMS)_3$ (M = Ru, Os). Theory of the Paramagnetic Shift for Strong Field d^5 Complexes

B. R. McGarvey,* N. C. Batista, C. W. B. Bezerra, M. S. Schultz, and D. W. Franco

Instituto de Química de São Carlos, Universidade de São Paulo, São Carlos, SP, Brazil

Received November 14, 1997

The EPR spectra of $[Ru(NH_3)_5(H_2O)](TFMS)_3$ and $[Os(NH_3)_5(H_2O)](TFMS)_3$ (TFMS = trifluoromethanesulfonate) have been measured for a range of temperatures for the solid powders and frozen solutions. The $g_{||}$ axis for the "axial" spectrum observed is shown to be perpendicular to the M−O bond axis, as it is perpendicular to the antibonding MO that interacts in a π fashion with the water molecule. The ^{1}H NMR of both compounds in 1,2-propanediol carbonate has been obtained over a range of temperatures, and the resonances for axial ammonia, equatorial ammonia, and the bound water in the complex cation have been identified. Using the experimental g values obtained from EPR and an improved equation that uses all t_2 states, the dipolar component of the shift has been calculated and used to find the contact portion of the paramagnetic shift. An improved equation for the contact shift has been developed which separates the spin contribution into the d_{xz}, d_{yz}, and d_{xy} portions and this theory applied to the measured contact shifts. Values for three hyperfine constants have been obtained, the $A(NH_3)$ constant for the MOs that do not π interact with the water molecule, the $A(NH_3)$ constant for the MO that does π interact, and the $A(H_2O)$ for the MO that does π interact. The spin transfer for the ammonia ligand protons is by hyperconjugation giving a positive A, and for the water proton it is mainly by covalent transfer of spin to the nonbonding p orbital with polarization of the spin on the proton giving a negative A.

I. Introduction

The strong field d^5 complexes are well situated for combined theoretical and experimental studies. At low temperatures, the EPR can be detected giving valuable information concerning the properties and nature of the ground state while, at higher temperatures, the paramagnetic shift can be measured giving information on the small hyperfine interactions between the spin in the antibonding molecular orbitals and the ligand nuclei. One of the authors, B. R. McGarvey, has had serious misgivings about the theories of the paramagnetic shift and their applications for these complexes. As it turned out there were also problems with the theories, or at least in their application to experiment, for the **g** matrix which made it even more difficult to revise the paramagnetic shift equations in a manner that was better but still easy to apply to experimental systems.

Much of the EPR and NMR work on strong field d^5 complexes has been done on Fe^{3+} systems, but the only simple and small complexes of Fe^{3+} that are strong field are the cyanides, so the bulk of the work has been done on the more complex, but interesting, porphyrins, phthalocyanines, hemoglobins, etc. To test a new theoretical approach, however, it is much better to start with smaller and simpler systems. It seemed to us that the Ru^{3+} and Os^{3+} complexes were better systems to start with. By now there exist a large number of small complexes, all strong field, of these ions that have been made and characterized, but no serious study of the nature of the paramagnetic shift has been undertaken with them.

Bleaney and O'Brian[1] were the first to explain the nature and properties of the g matrix in these strong field d^5 systems. Since then, a large number of variations of their original equations and methods of applying them have appeared[2−19] but unfortunately there were many mistakes in the equations and in their application. This has been reviewed[20,21] recently and a new simplified approach to applying the correct equations proposed.

In this work we will be extending an approach to the paramagnetic shift that has been applied[22] successfully to the tetrahedral Co^{2+} and Ni^{2+} complexes and more recently[23] to the actinium tetrakis(methyl borohydrides). Previous approaches

* To whom correspondence should be addressed. Permanent address: Department of Chemistry and Biochemistry, University of Windsor, Windsor, Ontario N9B 3P4, Canada.

(1) Bleaney, B.; O'Brien, M. C. M. *Proc. Phys. Soc. (London)* **1956**, *69*, 1216.
(2) Thornley, J. M. H. *Proc. Phys. Soc. C* **1968**, *1*, 1024.
(3) Hudson, A.; Kennedy, M. J. *J. Chem. Soc. A* **1969**, 1116.
(4) Griffiths, J. S. *Mol. Phys.* **1971**, *21*, 135.
(5) Hill, N. J. *J. Chem. Soc., Faraday Trans. 2* **1972**, *68*, 427.
(6) DeSimone, R. E. *J. Am. Chem. Soc.* **1973**, *95*, 6238.
(7) Sakaki, S.; Hagiwara, N.; Yanase, Y.; Ohyoshi, A. *J. Phys. Chem.* **1978**, *82*, 1917.
(8) Sakaki, S.; Yanase, Y.; Hagiwara, N.; Takeshita, T.; Naganuma, H.; Ohyoshi, A.; Ohkubo, K. *J. Phys. Chem.* **1982**, *86*, 1038.
(9) Gupta, H. K.; Dikshit, S. K. *Polyhedron* **1987**, *6*, 1009.
(10) Bohan, T. *J. Magn. Reson.* **1977**, *26*, 109.
(11) Taylor, C. P. S. *Biochim. Biophys. Acta* **1977**, *491*, 137.
(12) Reiff, W. M.; DeSimone, R. E. *Inorg. Chem.* **1973**, *12*, 1793.
(13) Kaplon, D.; Navon, G. *J. Phys. Chem.* **1974**, *78*, 700.
(14) Cotton, S. A.; Gibson, J. F. *J. Chem. Soc. A* **1971**, 803.
(15) Medina, A. N.; Gandra, F. G.; Baesso, M. L.; Lima, J. B.; McGarvey, B. R.; Franco, D. W. *J. Chem. Soc., Faraday Trans.* **1997**, *93* (11), 2105.
(16) DeSimone, R. E.; Drago, R. S. *J. Am. Chem. Soc.* **1970**, *92*, 2343.
(17) Merrithew, P.; Lo, C.-C.; Modestino, A. J. *Inorg. Chem.* **1973**, *12*, 1927.
(18) LaChance-Galang, K. J.; Doan, P. E.; Clarke, M. J.; Daghlian, H.; Rao, U.; Yamana, A.; Mandal, S.; Hoffman, B. M. *J. Am. Chem. Soc.* **1995**, *117*, 3529.
(19) Ezzeh, C.; McGarvey, B. R. *J. Magn. Reson.* **1974**, *15*, 183.
(20) McGarvey, B. R. *Quim Nova* **1998**, *21*, 206.
(21) McGarvey, B. R. *Coord. Chem. Rev.*, in press.
(22) McGarvey, B. R. *Inorg. Chem.* **1995**, *34*, 6000.
(23) McGarvey, B. R. *Inorg. Chim. Acta*, in press.

S0020-1669(97)01439-0 CCC: $15.00
Published on Web 06/15/1998

to the paramagnetic shift assumed the shift of a given nucleus was proportional to the total spin of the paramagnetic ion. This new approach partitions the spin into those portions belonging to different d orbitals and assumes the shift of a given nucleus is only proportional to that spin which belongs to d orbitals of appropriate symmetry. This seems an obvious thing to do, but the approach never seems to have been applied to those systems in which the d orbitals and their spins are mixed up by the spin−orbit interaction. In the transition metals this applies to all systems which have, or are close to having, a T_2 or T_1 ground state.

We have found only a few serious studies of the paramagnetic shift in Ru^{3+} complexes. Waysbort and Navon[24] have reported detecting the paramagnetic shift of the coordinated ammonia ligand in $[Ru(NH_3)_6]^{3+}$ ion in water solutions over an interval of temperatures in their study of proton exchange with the solvent molecules but only used it to explain the shift in the water resonance with pH. Three related papers[18,25,26] have reported on EPR and NMR studies of $[L(NH_3)_5Ru]^{3+}$ and *cis*- and *trans*-$[LL'(NH_3)_4Ru]^{3+}$ complexes. The *g* values obtained from EPR were used to estimate the dipolar component of the shift, and the contact shift was obtained by subtracting this dipolar shift from the measured shift. These studies were concerned only with the shifts in the conjugated ligands L and L′; they presumably did not measure the ammonia peaks since no shifts were reported. The studies did not attempt to obtain hyperfine constants from the contact shifts but were concerned only about the sign and relative magnitudes of the hyperfine constants.

For our first system to study we have chosen the $[Ru(NH_3)_5(H_2O)]^{3+}$ and $[Os(NH_3)_5(H_2O)]^{3+}$ ions. Although this system seems simple enough, it turns out to present a few complications as we shall see below.

II. Experimental Section

A. Synthesis. The compounds $[Ru(NH_3)_5(H_2O)](TFMS)_3$[27] and $[Os(NH_3)_5(H_2O)](TFMS)_3$[28] (TFMS = trifluoromethanesulfonate) were prepared by literature methods and checked by UV−visible−IR spectroscopic methods and electrochemical techniques.

B. EPR Spectra. The spectrometer was a Bruker ESP 300e equipped with a variable-temperature accessory and a liquid N_2 dewar insert. The magnet was capable of field sweeps as high as 1.4 T.

It was found difficult to get a good simulation of powder spectra using the Bruker Simfonia program, for the large range of *g* values observed, so a simulation program was written that incorporates two features not found in the commercial program. The first feature was to include a *g* factor dependence in the broadening function's line width. The Gaussian and Lorentzian functions are really for the frequency domain and the line width parameters are frequency line widths while the EPR spectra are run at constant frequency. Therefore, the line widths in the field domain are inversely dependent on the *g* value. This becomes important when the *g* value ranges from 3 to 0, as it does in the systems studied here.

The second feature added was to recognize that the intensity from a given crystallite in the powder pattern was not constant for all orientations of the magnetic field but was dependent upon the square of the *g* value perpendicular to the field direction along the direction of the B_1 oscillating field of the microwave cavity. We can account for this intensity variation by including an intensity factor, which is given by the equation

$$\frac{3\{g_x^2 + g_y^2 + [g_z^2 - (g_x^2\cos^2\phi + g_y^2\sin^2\phi)]\sin^2\theta\}}{2(g_x^2 + g_y^2 + g_z^2)} \quad (1)$$

Including these two features produces a simulated spectrum that can be very close to the experimental spectrum.

A simulation program has also been written that uses the simplex algorithm to do an automatic least-squares fitting of the three *g* value plus three line width parameters. Although the program is slow (taking a couple hours on a 100 MHz PC), it does find the best fit quite reliably. A figure (Figure S1) demonstrating the excellence of the simulations obtained is deposited as Supporting Information. It is for the EPR spectrum of the $[Ru(NH_3)_5(H_2O)](TFMS)_3$ solid at 156 K.

C. NMR. The NMR spectra were taken at the Departamento de Química, Universidade Federal do São Carlos, on a Bruker Advance DRX 400 spectrometer which was equipped with a EuroTherm BVT2000 variable-temperature accessory.

III. Theory

A. g Matrix. We start with the revised and corrected theory for the **g** matrix of strong field d^5 systems that are slightly distorted from octahedral symmetry, which has recently been the subject of two reviews.[2,3] This treatment uses the $|l,s\rangle$ basis functions

$$\left|-1,\pm\frac{1}{2}\right\rangle = d_1^{+}d_1^{-}d_{xy}^{+}d_{xy}^{-}d_{-1}^{\pm}$$
$$\left|+1,\pm\frac{1}{2}\right\rangle = d_{-1}^{+}d_{-1}^{-}d_{xy}^{+}d_{xy}^{-}d_1^{\pm}$$
$$\left|0,\pm\frac{1}{2}\right\rangle = \pm i d_1^{+}d_1^{-}d_{-1}^{+}d_{-1}^{-}d_{xy}^{\pm} \quad (2)$$

in which the sign convention plus use of the imaginary number *i* were chosen to give two identical and real 3 × 3 spin−orbit matrixes. If H_C is the crystal or ligand field operator, the Δ and *V* parameters are defined in terms of the one electron matrix elements

$$\langle d_{xy}|H_C|d_{xy}\rangle = \Delta \quad \langle d_{xz}|H_C|d_{xz}\rangle = \frac{V}{2} = -\langle d_{yz}|H_C|d_{yz}\rangle \quad (3)$$

Using these definitions and the spin−orbit interaction operator H_{LS}

$$H_{LS} = \sum_i \xi(l_i s_i) \quad (4)$$

we obtain the determinant

$$\begin{vmatrix} \left|-1,\frac{1}{2}\right\rangle & \left|0,-\frac{1}{2}\right\rangle & \left|+1,\frac{1}{2}\right\rangle \\ \left|+1,-\frac{1}{2}\right\rangle & \left|0,\frac{1}{2}\right\rangle & \left|-1,-\frac{1}{2}\right\rangle \\ \left(2\Delta - \frac{1}{2}\xi - E\right) & -\frac{\xi}{\sqrt{2}} & \frac{V}{2} \\ -\frac{\xi}{\sqrt{2}} & (\Delta - E) & 0 \\ \frac{V}{2} & 0 & \left(2\Delta + \frac{1}{2}\xi - E\right) \end{vmatrix} = 0 \quad (5)$$

The wave functions for the Kramer's doublet ground state are chosen to be

$$\psi_+ = a\left|+1,-\frac{1}{2}\right\rangle + b\left|0,\frac{1}{2}\right\rangle + c\left|-1,-\frac{1}{2}\right\rangle$$
$$\psi_- = a\left|-1,\frac{1}{2}\right\rangle + b\left|0,-\frac{1}{2}\right\rangle + c\left|+1,\frac{1}{2}\right\rangle \quad (6)$$

Neglecting spin−orbit admixtures with the excited states (t_2^4e, etc.), the principal *g*-values can be calculated from the Zeeman interaction,

(24) Waysbort, D.; Navon, G. *J. Phys. Chem.* **1973**, *77*, 960.
(25) Clarke, M. J.; Bailey, V. M.; Doan, P. E.; Hiller, C.; LaChance-Galang, K. J.; Daghlian, H.; Mandal, S.; Basto, C.; Lang, D. *Inorg. Chem.* **1996**, *35*, 4896.
(26) Rodriguez-Bailey, V. M.; LaChance-Galang, K. J.; Doan, P. E.; Clarke, M. J. *Inorg. Chem.* **1997**, *36*, 1873.
(27) Krenztian, H. Mixed Valence Ruthenium Ammine Dinitrile and Related Complexes. Ph.D. Thesis, Stanford University, 1976.
(28) Lay, P. A.; Magnuson, R. H.; Taube, H. *Inorg. Chem.* **1989**, *28*, 3001.

$H_z = \beta \boldsymbol{B}(k\boldsymbol{L} + 2\boldsymbol{S})$, where k is the orbital reduction factor. The resulting principal g values are

$$g_x = -2[-2ac + b^2 + k\sqrt{2}b(a - c)]$$

$$g_y = -2[2ac + b^2 + k\sqrt{2}b(a + c)]$$

$$g_z = -2[a^2 - b^2 + c^2 + k(a^2 - c^2)] \quad (7)$$

The earlier mentioned review[2] pointed out that if we assign the labels of x, y, and z such that Δ and V have the same sign and $V/\Delta \leq {}^2/_3$, it is a simple matter to solve the above equations plus the normalization condition for a, b, c, and k, and from these the parameters of Δ/ξ and V/ξ can be obtained. With this convention, the three g values in order of decreasing magnitude can only have the order g_x, g_y, g_z or g_z, g_y, g_x. For both orders, the first two g values are negative and the lowest magnitude g can be plus or minus. When one solves the equations for the four assignments, one of the two orders gives a $V/\Delta > {}^2/_3$, leaving us to make a choice between only two possible solutions for the system. Often, an unrealistic value of either k or Δ makes our choice easy. The one trouble with this approach is the possibility that the labels you get for x, y, and z may not be what you might have guessed intuitively, and this turned out to be the case in the systems studied in this work.

B. Theory of the NMR Paramagnetic Shift. In this theory we start with the above equations for the g values and assume the values of Δ, V, and k have been obtained as outlined above from the g values of the ground state as determined by EPR, at low temperatures where the spin lifetime is long enough to make EPR measurements. Using these parameters plus ξ, eq 4 can be solved and the mixing coefficients (a_n, b_n, c_n) for the three Kramer's doublet states obtained, as well as the energies of these states.

The approach used here was successfully applied to the cases of tetrahedral Co^{2+} and Ni^{2+} complexes[22] and to methyl borohydride complexes of actinides[23] using the equations of Kurland and McGarvey:[29]

$$\left(\frac{\Delta\nu}{\nu_0}\right)_i = -q^{-1}\left\{\sum_{\Gamma n,\Gamma' m} Q_{\Gamma\Gamma'}\langle\Gamma n|\mu_i|\Gamma' m\rangle\left\langle\Gamma' m\left|\frac{(A_N)_i}{\gamma\hbar}\right|\Gamma n\right\rangle\right\} \quad (8)$$

$$q = \sum_{\Gamma n} e^{-E_\Gamma/kT} \quad (9)$$

$$Q_{\Gamma\Gamma'} = \frac{\{e^{-E_\Gamma/kT} - e^{-E_{\Gamma'}/kT}\}}{(E_\Gamma - E_{\Gamma'})} \quad (10)$$

$$\mu_i = \beta(L_i + 2S_i)_i \quad (11)$$

In the above equations i is x, y, or z, E_Γ is the energy of the three Kramer's doublets before the application of the magnetic field B_0, and n and m refer to the different wave functions of the doublet. $[(A_N)_i/\gamma\hbar]$ is the hyperfine interaction operator in units of gauss, whose form will be discussed below when we consider different components of the shift. The other symbols have their usual meaning. Equation 8 is a condensed form of the equation given by Kurland and McGarvey.[29] They separated out the terms in which $(E_\Gamma - E_{\Gamma'}) = 0$ which have a special limiting form. The above form is more amenable to programming in a computer which has a subroutine to handle all possible values of $\Delta E = (E_\Gamma - E_{\Gamma'})$.

1. Dipolar or Pseudocontact Shift. This is the long range component contributed by electrons centered on the paramagnetic metal ion arising from the anisotropy of the magnetic moment of the ion, which prevents the dipolar field from being averaged out by the tumbling motion of the complex in solution. This is a particularly large shift in the strong field d^5 complexes due to the large anisotropy in the **g** matrix of these complexes. McGarvey and Kurland[29] have shown that it assumes the simple form

$$\left(\frac{\Delta\nu}{\nu_0}\right) = {}^1/_3[\chi_{zz} - {}^1/_2(\chi_{xx} - \chi_{yy})]\frac{(3\cos^2\theta - 1)}{R^3} + {}^1/_2[\chi_{xx} - \chi_{yy}]\frac{\sin^2\theta\cos 2\phi}{R^3} \quad (12)$$

where χ is the atomic magnetic susceptibility of the ion, and θ and ϕ are the polar angles giving the orientation of the distance vector R connecting the metal ion with the nucleus whose NMR is being measured. The atomic susceptibility χ can be calculated from the equations

$$\chi_i = -\frac{\beta^2}{4q}\sum_{\Gamma\Gamma' nm}(g_{nm})^2{}_i Q_{nm} \quad (13)$$

$$(g_{nm})_z = -2[a_n a_m - b_n b_m + c_n c_m + k(a_n a_m - c_n c_m)] \quad (14)$$

$$(g_{nm})_x = -2\left[-(a_n c_m + a_m c_n) + b_n b_m - \frac{k}{\sqrt{2}}(a_n b_m + a_m b_n - b_n c_m - b_m c_n)\right] \quad (15)$$

$$(g_{nm})_y = -2\left[(a_n c_m + a_m c_n) + b_n b_m + \frac{k}{\sqrt{2}}(a_n b_m + a_m b_n + b_n c_m + b_m c_n)\right] \quad (16)$$

2. Contact Shift. This part of the shift arises from spin transfer from the t_2 d orbitals of the metal ion into the orbitals of the ligand atom. The spin transfer mechanism could be a direct covalency interaction or an indirect polarization interaction. In the case of orbitally nondegenerate systems, the treatment of the hyperfine interaction has been fairly straightforward because we deal with a ground state in which there is a single d orbital that can interact only with specific ligand nuclei and has a clearly defined value of m_S for the spin. This is not the case here, where the ground state is a mixture of all three t_2 orbitals and a mixture of $m_S = \pm{}^1/_2$, as can be seen in eq 6. We shall assume that the hyperfine operator $[(A_N)_i/\gamma\hbar]$ in eq 7 is of the isotropic form $\sum_j A_j^k \mathbf{s}$, where j refers to the ligand nucleus and k to the d orbital. Thus when the operator is applied to for example the d_{xy} orbital the A_j^{xy} are zero for the two ligands on the z axis. Thus in eq 8 the shift for a given nucleus j will have three terms of $F_i(j,k)A_j^k$ and we will use eq 8 to calculate the $F_i(j,k)$ which give the partitioning of s_i among the d_k orbitals that could spin interact with the jth nuclear spin. This is not as difficult as it may sound, and after we average over three spatial components, we end up with just three functions, which we will label $F_{av}(xz)$, $F_{av}(yz)$, and $F_{av}(xy)$. $F_{av}(xz)$ and $F_{av}(yz)$ apply to ligands along the z axis, $F_{av}(xz)$ and $F_{av}(xy)$ to ligands along the x axis, and so forth. A computer program has been written to calculate these parameters and the susceptibility parameters appropriate to the dipolar shift. It was our hope in developing these equations that we could separate out the dipolar contribution to get the contact portion of the shift, and then division of the contact shift by the appropriate F_{av} term would give an estimate of A_j^k.

IV. Results

A. EPR of $[Ru(NH_3)_5(H_2O)](TFMS)_3$ and $[Os(NH_3)_5(H_2O)](TFMS)_3$. The EPR spectra of $[Ru(NH_3)_5(H_2O)](TFMS)_3$ and $[Os(NH_3)_5(H_2O)](TFMS)_3$ in the solid state and in frozen solutions were obtained at a variety of temperatures starting with liquid nitrogen. Figures 1 and 2A show the spectra of the solid ruthenium and osmium compounds, respectively, at different temperatures. The apparent decrease in intensity is due to increasing line breadth with temperature due to the

(29) Kurland, R. J.; McGarvey, B. R. *J. Magn. Reson.* **1970**, *2*, 286.

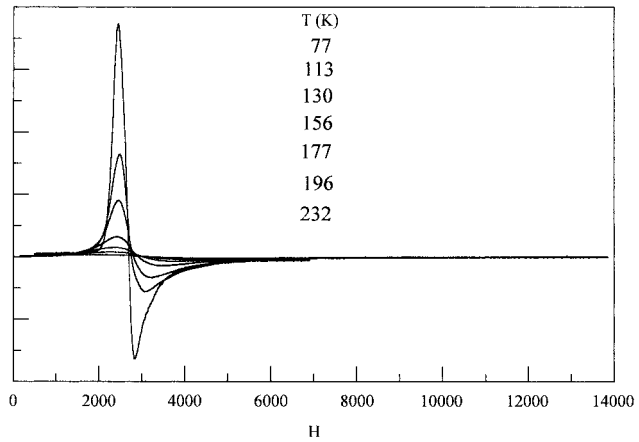

Figure 1. EPR spectra at different temperatures for $[Ru(NH_3)_5(H_2O)](TFMS)_3$ powder.

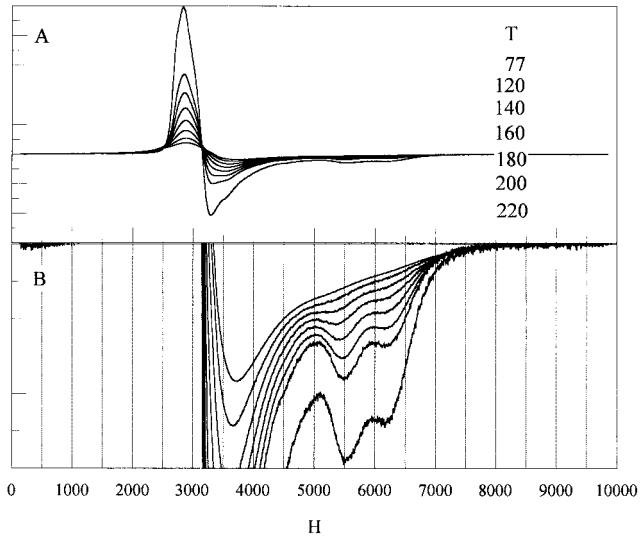

Figure 2. (A) EPR spectra at different temperatures for $[Os(NH_3)_5(H_2O)](TFMS)_3$ powder. (B) Increased gain to show two parallel peaks.

decrease in spin T_1. The integrated line intensity remains constant after being corrected for the expected Curie law dependence. No g parallel peak can be detected in $[Ru(NH_3)_5(H_2O)](TFMS)_3$ while two peaks are observed for $[Os(NH_3)_5(H_2O)](TFMS)_3$ (see Figure 2B). Tests with the simulation program show that the g parallel peak becomes impossible to detect when $g_{||} < 0.6$ due to the decreasing intensity of the peak and broadening associated with the small g values.

At 77 K the simulation of $[Ru(NH_3)_5(H_2O)](TFMS)_3$ solid gives $g_\perp = 2.620$ and $0.6 \geq g_{||} \geq 0$. The same values were obtained from frozen solutions in 1,2-propanediol carbonate and water. For $[Os(NH_3)_5(H_2O)](TFMS)_3$ solid the simulation was difficult due to the presence of two signals that resolved only in the $g_{||}$ region. We are fairly certain that at 77 K one signal has $g_\perp = 2.3$ and $g_{||} = 1.22$ and the other has $g_\perp = 2.2$ and $g_{||} = 1.08$. The two $g_{||}$ peaks were also observed in frozen water solutions, so the two signals are not a crystalline-state phenomena. Also the same spectrum occurred in different preparations of the compound, so the double spectrum is a feature of the pure molecule. The simulations were done by assuming equal amounts of both species, but it became apparent that better results would have been obtained if we had assumed the peak with the smaller $g_{||}$ to be somewhat less than 50%.

Using the equations given in section IIIA, we obtain $V = 0$ for both systems, naturally, and the values of $0.71 \leq \Delta/\xi \leq 1.36$ and $1.05 \leq k \leq 0.97$ for $[Ru(NH_3)_5(H_2O)](TFMS)_3$ and $\Delta/\xi = 0.39, 0.41$ and $k = 0.98, 0.90$ for the two forms of $[Os(NH_3)_5(H_2O)](TFMS)_3$. Using the nominal values of $\xi = 1000$ cm^{-1} for Ru^{3+} and 3000 cm^{-1} for Os^{3+} the two values for Δ are similar for the two compounds. In the analysis of the NMR of the ruthenium compound, we will use the values of Δ and k obtained from both $g_{||} = 0$ ($\Delta = 990$ cm^{-1} and $k = 0.97$) and $g_{||} = 0.6$ ($\Delta = 710$ cm^{-1} and $k = 1.05$).

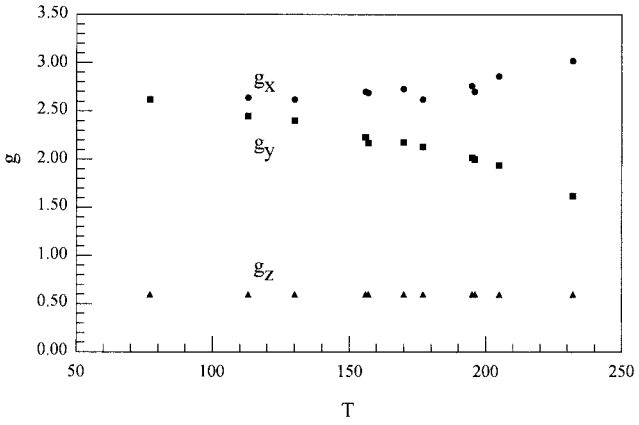

Figure 3. Variation of g_x and g_y with temperature for $[Ru(NH_3)_5(H_2O)](TFMS)_3$ powder. They were determined by a least-squares simulation keeping g_z fixed at 0.60.

For reasons that will be discussed below, we decided to simulate the spectra at higher temperatures to examine any changes in g with temperature. In Figure 3 are plotted the g values for the solid for $[Ru(NH_3)_5(H_2O)](TFMS)_3$. The smallest g value was fixed in the simulation because its value has no effect on the spectrum as long as it is kept small enough. The line width increases with temperature due to the shortening of the spin T_1, but to get a good simulation it was necessary to make the line width associated with the intermediate g value several hundred gauss larger than the others at the higher temperatures. The central g value moves so much that the Δ/ξ value switches from plus to minus at the highest temperatures. For the frozen solution of $[Ru(NH_3)_5(H_2O)](TFMS)_3$ in 1,2-propanediol carbonate the behavior is different in that the two largest g values remain essentially equal and constant with temperature, only the line width increases as the temperature is increased.

Although simulation is hard for the solid $[Os(NH_3)_5(H_2O)](TFMS)_3$, the shape in the $g_\perp$ region at some temperatures indicates something similar is occurring in this compound. It can also be seen in Figure 2B that one of the $g_{||}$ peaks moves to higher values as the temperature increases, resulting in better resolution of the two peaks even though the line widths are increasing. The EPR of this compound has been reported before for liquid-He temperatures.[15] The average of the two $g_\perp$ values is smaller at liquid He than at liquid N_2, and the reverse is true for the $g_{||}$ average. Either the g values move away from 2.00 as the temperature goes from 4 to 77 K or one $g_{||}$ and $g_\perp$ remain nearly constant while the other two move away from 2.00 and cross the other g values. We cannot tell which is the case until a variable-temperature study is done between 4 and 77 K. Despite this movement of the g values, the value of Δ/ξ at 4 K is only slightly smaller than what we found at 77 K.

B. Proton NMR of $[Ru(NH_3)_5(H_2O)](TFMS)_3$. The compound is soluble in water, but we wished to avoid this solvent because we feared there would be rapid proton exchange with the solvent, at least for the coordinated water molecule, and this fear was justified. The compound was found to be soluble

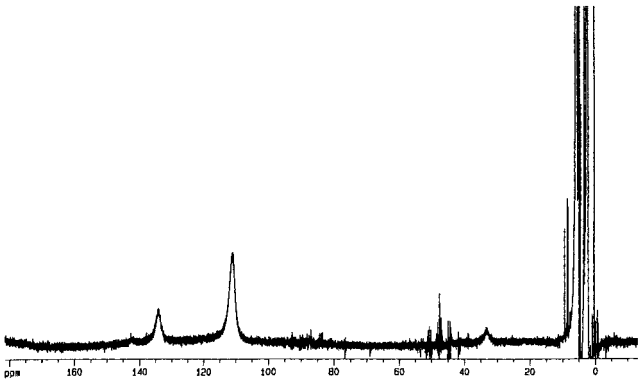

Figure 4. Proton NMR of $[Ru(NH_3)_5(H_2O)](TFMS)_3$ in 1,2-propanediol carbonate at 50 °C measured at 400 MHz. The peaks between 0 and 10 ppm are solvent peaks plus residual water from the solvent. From left to right the three broad downfield peaks have been identified as axial ammonia, equatorial ammonia, and water, respectively.

in 1,2-propanediol carbonate, and if the contamination of the solvent with water was kept small enough, we were able to detect two downfield ammonia peaks and one water peak as can be seen in Figure 4 taken at 323 K. The line width of these broad peaks increased even more at the lower temperatures. Spectra were taken from −40 to 90 °C, but it was found that a reaction took place between the solvent and the solute between 70 and 90 °C turning the colorless solution bright red. Even at room temperature the solution turned pink after a day or so. The axial ammonia peak became too broad to detect at −40 °C, and the bound water peak disappeared above 50 °C due presumably to its averaging with the residual water peak in the solution.

The paramagnetic shifts of the ammonia resonances were referenced internally to one of the solvent peaks to compensate for internal fields from the paramagnetic susceptibility of the solution. This was then corrected to reference the shift against the shifts of 2.57, 2.91 ppm in diamagnetic $[Ru(NH_3)_5(H_2O)]^{2+}$. We used the average of 2.7 as our diamagnetic reference for both ammonia shifts since the error in the measurement of the shifts varied from ± 0.3 to ± 2 ppm as the temperature decreased. The residual water peak in 1,2-propanediol carbonate was found at 2.91 ppm, and this was used as our diamagnetic reference as we had no value for the bound water peak in the diamagnetic $[Ru(NH_3)_5(H_2O)]^{2+}$. The error in the water peak shift varied from ±0.3 at the highest temperature to ±4 at the lowest temperature, so our estimate of the diamagnetic reference shift is probably accurate enough. The paramagnetic shifts are plotted in Figure 5 against the reciprocal of the absolute temperature.

C. Proton NMR of $[Os(NH_3)_5(H_2O)](TFMS)_3$. The results are similar to that in the ruthenium compound, and the spectrum observed at 16 °C is shown in Figure 6. The more intense unsymmetrical peak at 115 ppm contains the trans and equatorial ammonia peaks separated by 10 ppm. The two peaks are resolved at higher temperatures as the line widths become narrower. The lowest temperature at which we could detect the resonance lines was −33 °C, and the highest temperature was 67 °C when overheating of the probe forced the stop of the experiment. At the highest two temperatures, additional small resonances appeared in the 90−150 ppm region, which along with the appearance of a pink color indicated that a reaction was proceeding between the solute and the solvent, just as was observed in the ruthenium compound. The shifts are plotted in Figure 7 versus the reciprocal temperature.

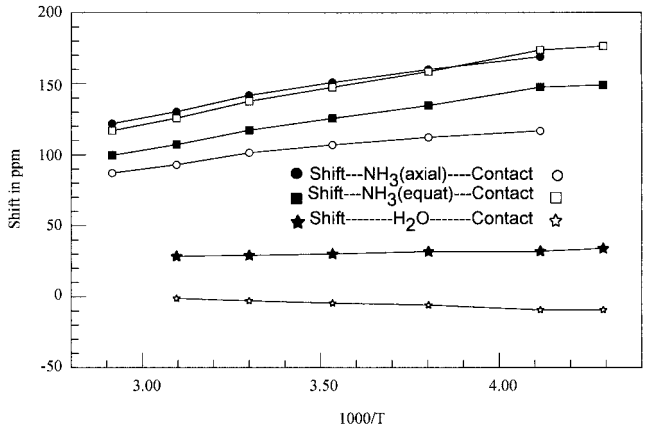

Figure 5. NMR paramagnetic shift of the three proton peaks in $[Ru(NH_3)_5(H_2O)]^{3+}$ in 1,2-propanediol carbonate as a function of the reciprocal Kelvin temperature given by the filled symbols. The open symbols show the contact shifts after correction for the dipolar component, obtained as explained in the text.

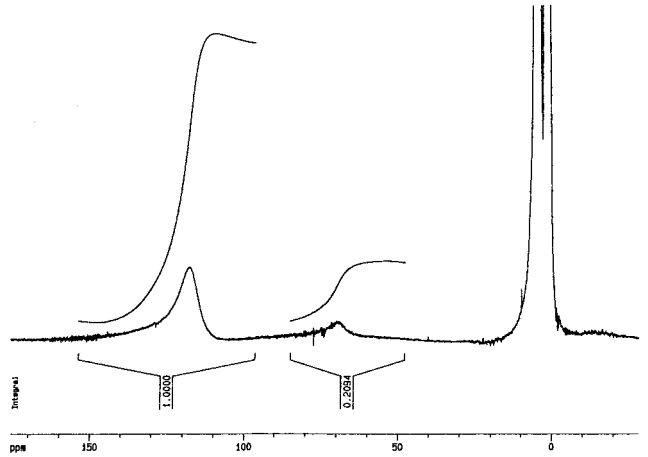

Figure 6. Proton NMR of $[Os(NH_3)_5(H_2O)](TFMS)_3$ in 1,2-propanediol carbonate at 16 °C measured at 400 MHz. The peaks between 0 and 10 ppm are solvent peaks plus the residual water from solvent. The asymmetrical more intense peak furthest downfield resolves into two separate peaks about 10 ppm apart at higher temperatures. As for the ruthenium compound, the three peaks are axial ammonia, equatorial ammonia, and water from left to right.

V. Discussion

A. Orientation of the $g_{||}$ Axis in the Complex Ion. When we first attacked this problem we fell into a trap by assuming the $g_{||}$ axis observed in the solid-state EPR was the M−OH_2 axis of the complex. Certainly this is a high-symmetry axis in solution as evidenced by the NMR, which shows four equivalent equatorial ammonia resonances and a separate resonance for the single trans ammonia. Unfortunately this assumption forces us to reach certain untenable conclusions from our results. The first untenable conclusion comes from the positive value of Δ, which means that the one electron energy for d_{xy} is about 1000 cm^{-1} above the $d_{xz,yz}$ orbitals. This is unreasonable since the splitting of the t_2 orbitals is due to π bonding, and the only sizable π bonding would come from the nonbonding electrons of oxygen in the water molecule which is on the z axis.

The second untenable conclusion comes when we try to calculate the contact shift for the two types of ammonia protons. If we take $g_{||}$ axis to be the M−O axis, then $(\chi_{||} - \chi_{\perp})$ is negative and the dipolar shift for the axial ammonia will be large and upfield while the shift for the equatorial ammonias will be downfield. This will place the axial contact shift in the 200−

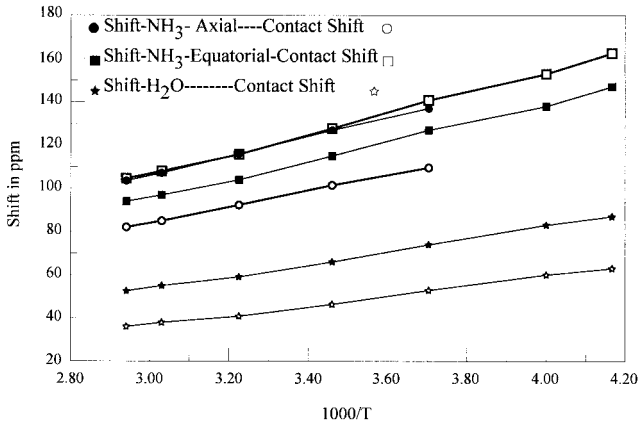

Figure 7. NMR paramagnetic shift of the three proton peaks in $[Os(NH_3)_5(H_2O)]^{3+}$ in 1,2-propanediol carbonate as a function of the reciprocal Kelvin temperature given by the filled symbols. The open symbols show the contact shifts after correction for the dipolar component, obtained as explained in the text.

300 ppm range and the equatorial shifts near 50 ppm. This is an unreasonable result for a system in which the unpaired electron is supposed to be mainly in a d_{xy} orbital.

The answer[30] to this problem comes when we recognize that in EPR we are dealing with a rigid system in which the water molecule is fixed in space. Only the electron pair in the oxygen atom perpendicular to the water molecule plane can π donate into the one t_2 orbital that can π bond with this oxygen orbital. Thus the antibonding orbital involving this t_2 orbital is raised above the other two and the major distortion axis, $g_{||}$, is perpendicular to the plane of this orbital and therefore perpendicular to the M−O bond direction. Of course, in solution the water molecule rotates about the M−O axis, which means the $g_{||}$ axis rotates also, giving rise to a symmetry axis about M−O in which the $g_{||}$ and $g_{\perp}$ average to give a new $g_{\perp}$ in the equatorial plane while the old $g_{\perp}$ along the M−O direction becomes the new $g_{||}$.

This could explain the variation in g with increasing temperature observed for solid $[Ru(NH_3)_5(H_2O)](TFMS)_3$. There could be a partial averaging of the two g's in the equatorial plane due to some motion associated with the orientation of the water molecule. The existence of two resonances in $[Os(NH_3)_5(H_2O)](TFMS)_3$ could be due to two different orientations of the water molecule in which a variation in the lattice fields for the two orientations could produce two slightly different g values. This new orientation of the axis will be shown below to predict more reasonable contact shifts for the ammonia protons.

It should be pointed out that this location of the major distortion g axis perpendicular to the bonding axis of a ligand that π bonds only in one plane has been postulated before.[18,25,26,31] In these cases, the ligand was an aromatic ligand and not the simple water molecule. The value of Δ obtained here from the g values is a direct measure of the value for the angular overlap model, AOM, parameter of ϵ_π for H_2O. Our results also demonstrate that the π interaction involves only one of the two d orbitals that could π interact with the oxygen atom.

B. NMR of [(Ru, Os)$(NH_3)_5(H_2O)](TFMS)_3$. The shifts shown in Figures 5 and 7 are the sum of the contact shift and the dipolar or "pseudocontact" shift, so we first need to estimate the dipolar shift using eqs 12−16. Here we have a problem in that the parameters we use in the calculation are for a rigid molecule in which the distortion axis in the **g** matrix is perpendicular to the M−O axis. Presumably in solution, the water molecule is rotating rapidly about the M−O axis producing an average. Our problem is what model do we use to represent this rotation? After some consideration of the problem, we have opted for the free rotation model in which the $g_{||}$ axis is assumed to take all possible orientations in the equatorial plane of the complex ion. We have chosen this model because we believe there is only a small barrier to rotation of the water molecule within the complex itself. The essential C_4 symmetry of the rest of the complex ion allows π bonding for any orientation. We have tried some possible jump models, but the results are not that different, in the end.

For our calculations we will label the $g_{||}$ axis as the z axis and recognize that it is perpendicular to the antibonding MO and therefore is in the plane of the H_2O molecule and perpendicular to the M−O axis. We will call the M−O axis the x axis.

If we assume rotation of NH_3 about the M−N bond and this bond makes an angle κ with the $g_{||}$ axis, we can write

$$\frac{(3\cos^2\theta - 1)}{R^3} = \frac{(3\cos^2\kappa - 1)(3\cos^2\gamma - 1)}{2R^3} \quad (17)$$

where R is the distance between the metal ion and the proton on NH_3 and γ is the angle between the **R** vector and the M−N bond. For the axial ammonia $\kappa = 90°$ for all the orientations in the rotation of the $g_{||}$ axis, so it is not affected by the rotation of the water molecule within the complex. For the equatorial ammonia molecules we take the average of $(3\cos^2\kappa - 1)$ to be $^1/_2$ in eq 17. In the case of H_2O, the $g_{||}$ axis rotates with the water molecule so that $\theta = (90° - \gamma)$ at all times. In the calculation of the dipolar term we have used $R_{RuN} = 2.105$ Å,[18] $R_{OsN} = 2.113$ Å,[32] and $R_{NH} = 1.06$ Å. For simplicity we took $R_{MO} = R_{MN}$. When the calculated dipolar shift is subtracted from the experimental shift, we have the contact shift, which is plotted in Figures 5 and 7. The contact shifts shown in Figure 5 were calculated using parameters obtained from assuming $g_{||} = 0.0$ for the ruthenium compound. Using values from assuming $g_{||} = 0.6$ gave a dipolar shift 2 ppm smaller for the equatorial ammonia resonances and 4 ppm smaller for the axial ammonia and water resonances. These dipolar shifts are quite large, and applying the correction inverts the order of the shifts with the contact equatorial shift for ammonia being larger than the contact axial shift for ammonia. The correction also changes the sign of the shift for the water peak in the ruthenium complex.

In most treatments[18] of the dipolar shift, it has been assumed that one can ignore the excited states and use only the ground-state contribution as given by the equation

$$\frac{\Delta\nu}{\nu_0} = \left(\frac{\beta_e^2 S(S+1)}{9kT}\right)\left\{\left[g_z^2 - \frac{1}{2}(g_x^2 + g_y^2)\right]\frac{(3\cos^2\theta - 1)}{R^3} + \frac{3}{2}(g_x^2 - g_y^2)\frac{\sin^2\theta\cos 2\phi}{R^3}\right\} \quad (18)$$

Since our program also calculates this quantity, we can easily establish the error in ignoring the excited states in calculating the dipolar shift. In the case of the complex the error varied

(30) B.R.M. thanks Professor C. E. Schäffer, University of Copenhagen, Copenhagen, Denmark, for useful discussions that pointed us in the correct direction.

(31) Byrn, M. P.; Katz, B. A.; Kader, K. R.; Levan, K. R., Magurany, C. J.; Miller, K. M.; Pritt, J. W.; Strouse, C. E. *J. Am. Chem. Soc.* **1983**, *105*, 4916.

(32) Hambley, T. W.; Lay, P. A. *Inorg. Chem.* **1986**, *25*, 4553.

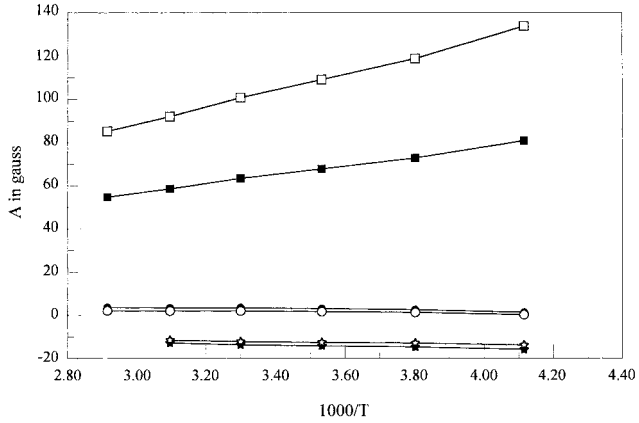

Figure 8. Hyperfine parameters as defined in the text for $[Ru(NH_3)_5(H_2O)]^{3+}$. The square symbols are for $A^{yz}_{NH_3}$, the circles are for $A^{xy}_{NH_3}$, and the stars are for $A^{xy}_{H_2O}$. The closed symbols were obtained by assuming $g_{||} = 0.0$ for the solid compound, and the open circles were obtained by assuming 0.60 for $g_{||}$.

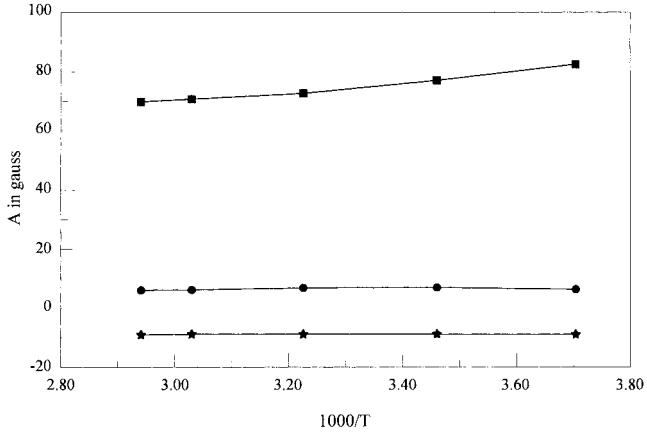

Figure 9. Hyperfine parameters as defined in the text for $[Os(NH_3)_5(H_2O)]^{3+}$. The square symbols are for $A^{yz}_{NH_3}$, the circles are for $A^{xy}_{NH_3}$, and the stars are for $A^{xy}_{H_2O}$.

from 13% to 21% from the lowest to the highest temperature and for the osmium compound the error varied from 6% to 8%. In all cases, eq 18 calculated a larger shift in magnitude. The main reason for the difference from eq 18 is in the Zeeman mixing terms between the ground state and the excited states which do not depend on the thermal population of the excited state but are a function of Δ/ξ.

Using the methods explained earlier in section IIIB2, we can write for the three contact shifts

$$\text{contact shift of } H_2O = F_{av}(xy)A^{xy}_{H_2O} + F_{av}(xz)A^{xz}_{H_2O} \quad (19)$$

$$\text{contact shift of axial } NH_3 = F_{av}(xy)A^{xy}_{NH_3} + F_{av}(xz)A^{xz}_{NH_3} \quad (20)$$

$$\text{contact shift of equatorial } NH_3 = 0.5F_{av}(xy)A^{xy}_{NH_3} + 0.5F_{av}(xz)A^{xz}_{NH_3} + F_{av}(yz)A^{yz}_{NH_3} \quad (21)$$

$A^{yz}_{NH_3}$ is easily obtained from eqs 20 and 21. Symmetry makes $F_{av}(xz) = F_{av}(yz)$, and it seems reasonable to have $A^{xz}_{NH_3} = A^{yz}_{NH_3}$, which allows us to extract a value for $A^{xy}_{NH_3}$ from eq 20. We have assumed that $A^{xz}_{NH_3}$ and $A^{xz}_{H_2O}$ should be similar because, as will be discussed below, they result from the same spin transfer mechanism and used this assumption to extract $A^{xy}_{H_2O}$ from eq 19. This assumption should not seriously affect the value of $A^{xy}_{H_2O}$ because $F_{av}(xz)$ is 1 order of magnitude smaller than $F_{av}(xy)$. The values obtained in this fashion are plotted in Figures 8 and 9.

If the theory and all the approximations made to obtain the contact shifts were good, we should expect no temperature dependence in the hyperfine parameters. The temperature dependence observed in $A^{yz}_{NH_3}$ is due to the near temperature independence of $F_{av}(yz)$ when Δ/ξ is one or larger. It will be noticed in Figure 8 that the temperature dependence is noticeably less when the parameters appropriate to $\Delta/\xi = 0.71$ are used. We suspect that inclusion of configuration mixing of e_g orbitals allowed by the low C_{2v} symmetry would begin to correct this problem. It should be noted that the magnitude and signs of the hyperfine constants are very similar for both complexes. A word of caution concerning the gauss unit used here is in order. These are expressed in the proton system, not in the electron system used in EPR. If you wish to know the value of A as it would be measured in the EPR spectrum, you must multiply these values by $\gamma\hbar/g_e\beta_e$ which is 1.5192704×10^{-3} for the proton; thus even the largest A reported here is about 0.1 G in an EPR spectrum.

Since the d orbitals do not have any π interaction with the nitrogen in the ammonia ligand, it is reasonable to ask from where does the hyperfine interaction with the ammonia protons come? The answer lies in a mechanism that has sometimes been referred to as hyperconjugation. The NH bonds keep the protons well away from the nodal plane of the d orbital, and at least one of the three bonding MOs belongs to the same irreducible representation as the d orbital so a small but direct transfer of spin into the H s orbitals is possible, producing a positive hyperfine interaction. This same mechanism leads to the well-known large positive hyperfine constant observed in aromatic free radicals when π spins interact with protons in a methyl group. This same mechanism should operate in the case of $A^{xz}_{H_2O}$ where the protons lie in the plane of d_{xz}. The case of $A^{xy}_{H_2O}$ is different in that here there is a direct π interaction which results in the transfer of spin into an oxygen p orbital but this cannot be transferred into the hydrogen s orbital because it lies in the nodal plain of the p orbital as well as of the d orbital. It is well-known, again in aromatic free radicals, that there is a polarization mechanism that produces a measurable hyperfine interaction, but in this case the constant has a negative sign just as is observed here. Thus the signs we observe are completely consistent with known spin transfer mechanisms we expect will be operating in this system.

Waysbort and Navon[24] have reported the measurement of the paramagnetic shift for the ammonia ligand in $[Ru(NH_3)_6]Cl_3$ in water solutions for 2−57 °C. On average there should be no dipolar shift in this system so the measured shifts are contact only. Applying our method of analysis to their data gives $A_{NH_3} = 29$ G, which is constant over the temperature interval of the measurements. This should be compared to our values of $A^{yz}_{NH_3}$ and $A^{xy}_{NH_3}$. It is interesting to note that their value is approximately the average of the two A values we obtained. Apparently the π interaction in d_{xy} results in a reduction of $A^{xy}_{NH_3}$ and an increase in $A^{yz}_{NH_3}$.

The $A^{xy}_{NH_3}$ value is rather small in magnitude considering the significant amount of π covalency suggested by Δ. We think this is not evidence of a small transfer of spin to the oxygen atom but evidence of a reduced polarization of spin on the H atom due to the very high ionic character of the OH bond. It is

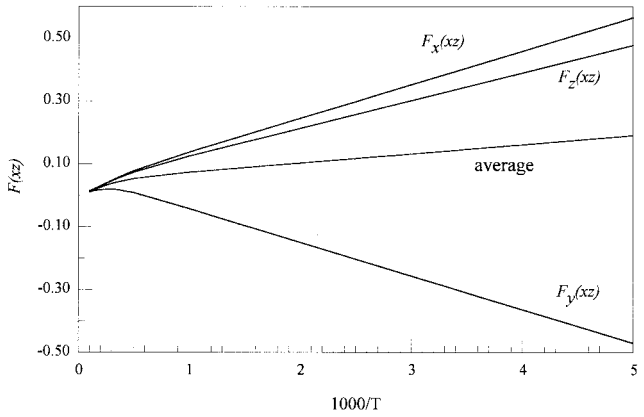

Figure 10. Calculated values of $F_i(xz)$ (defined in the text) for $[Os(NH_3)_5(H_2O)]^{3+}$ as a function of the reciprocal Kelvin temperature. The plot is shown to demonstrate the large anisotropy of the term. You get the same plot for $F_i(yz)$ except the subscripts for x and y are interchanged to preserve the axial symmetry of the complex ion.

known from the pK value[33] of this water molecule that the Ru^{3+} does increase the polarity of this bond significantly.

In our development of the equations for the contact shift we have assumed that the hyperfine interaction contains only the Fermi contact term, and for the proton NMR studied here, this is a reasonable assumption. If you were to apply our equations to nuclei in which there is a sizable dipolar contribution to the shift, $^{14,15}N$ for example, then there is a complication. The $F_i(j,k)$ values are very anisotropic, and therefore, the dipolar terms will not average out but will instead contribute to what we call the contact shift. This anisotropy is a result of the mixing up of spin and angular momentum states by the spin−orbit interaction. It is illustrated in Figure 10 where x, y, and z components of $F_i(j,k)$ are plotted against the reciprocal temperature for $[Os(NH_3)_5(H_2O)]^{3+}$. This means that if we were to measure the proton shifts for these systems in the solid state, we would find the contact shift to be anisotropic. Such an anisotropy has been detected in the ^1H NMR of uranacene.[34]

(33) Bezerra, C. W. B.; Gomes, M. G.; Silva, S. C.; Gambardella, M. T. P.; Santos, R. H.; Franco, D. W. Private communication.
(34) McGarvey, B. R.; Nagy, S. *Inorg. Chim. Acta* **1987**, *139*, 319; *Inorg. Chem.* **1987**, *26*, 4198.

VI. Conclusions

We have considered, above, the error incurred when using the standard eq 18 in evaluating the dipolar contribution to the shift and found that at most the error could be of the order of 20%. We did not address the errors incurred in applying the McConnell and Robertson[35] equation for contact shifts, which has the following form for $S = {}^1/_2$ systems

$$\frac{\Delta\nu}{\nu_0} = \frac{g_{av}\beta_e}{4kT}\frac{A}{\gamma\hbar} = F\frac{A}{\gamma\hbar} \tag{22}$$

For the $[Os(NH_3)_5(H_2O)]^{3+}$ example plotted in Figure 10, our F values at 300 K are between $^1/_4$ and $^1/_3$ of the F in eq 22. The F value in eq 22 is supposed to be the sum of all the F terms in the ion. At 300 K the sum of all three F values comes to about 47% of the value obtained from eq 22. Thus, large errors are to be expected if eq 22 is applied to the strong field d^5 ions, even in the high-symmetry complexes where only one hyperfine parameter is to be expected.

We have shown that the joint application of EPR and NMR spectroscopy to a simple strong d^5 metal complex is capable of extracting detailed information about the nature of the π interactions with ligands and the nature of the spin distribution in the neighboring ligands. The success of the theoretical approaches outlined above make it possible to mount an extensive study of related complexes, giving us specific parameters whose values can be compared and related to specific properties of the complexes. We hope to undertake such a task.

Acknowledgment. We wish to acknowledge the support of FAPESP (Proc. No. 97/6804-0) for this research. B.R.M. acknowledges the support of FAPESP (Proc. No. 97/6804-0) for his stay at the Institudo de Química de São Carlos, USP, which made possible any contributions he made to this work. We wish also to thank Alvickler Mangalhes for his assistance in taking the NMR spectra at the Departamento de Química, Universidade Federal do São Carlos.

Supporting Information Available: A figure comparing an experimental EPR spectrum to the simulated spectrum (1 page). Ordering information is given on any current masthead page.

IC9714394

(35) McConnell, H. M.; Robertson, R. E. *J. Chem. Phys.* **1958**, *29*, 1361.